

1
2
3
4
5
6
7
8
9
10
11
12
13
14
15
16
17
18
19
20
21
22
23
24
25
26
27
28
29
30

Denitrification in foraminifera has ancient origins and is complemented by associated bacteria

Christian Woehle^{1,5*}, Alexandra-Sophie Roy^{1*}, Nicolaas Glock^{2,6}, Jan Michels³, Tanita Wein^{1,7}, Julia Weissenbach^{1,8}, Dennis Romero⁴, Claas Hiebenthal², Stanislav N. Gorb³, Joachim Schönfeld², Tal Dagan¹

¹Institute of Microbiology, Kiel University, Am Botanischen Garten 11, Kiel, 24118, Germany

²GEOMAR Helmholtz Centre for Ocean Research Kiel, Wischhofstrasse, Kiel, 24148, Germany

³Zoological Institute, Kiel University, Am Botanischen Garten 1-9, Kiel, 24118, Germany

⁴Dirección General de Investigaciones Oceanográficas y Cambio Climático, Instituto del Mar del Perú, Callao 01, Peru 17

⁵Present address: Miltenyi Biotec B.V. & Co. KG, Friedrich-Ebert-Str. 68, Bergisch Gladbach, 51429, Germany

⁶Present address: Institute for Geology, University of Hamburg, Hamburg, 20146, Germany

⁷Present address: Department of Molecular Genetics, Weizmann Institute of Science, Rehovot 76100, Israel

⁸Present address: Faculty of Biology, Technion – Israel Institute of Technology, Haifa, 3200003, Israel

* Equally contributing authors

Corresponding authors: Christian Woehle woehle@gmail.com (C.W.), Tal Dagan tdagan@ifam.uni-kiel.de (T.D.)

31 **Summary**

32 Benthic foraminifera are unicellular eukaryotes that inhabit sediments of aquatic environments.
33 Several foraminifera of the order Rotaliida are known to store and use nitrate for denitrification,
34 a unique energy metabolism among eukaryotes. The rotaliid *Globobulimina* spp. has been
35 shown to encode an incomplete denitrification pathway of bacterial origins. However, the
36 prevalence of denitrification genes in foraminifera remains unknown and the missing
37 denitrification pathway components are elusive. Analysing transcriptomes and metagenomes
38 of ten foraminifera species from the Peruvian oxygen minimum zone, we show that
39 denitrification genes are highly conserved in foraminifera. We infer of the last common
40 ancestor of denitrifying foraminifera, which enables us to predict further denitrifying species.
41 Additionally, an examination of the foraminifera microbiota reveals evidence for a stable
42 interaction with *Desulfobacteracea*, which harbour genes that complement the foraminifera
43 denitrification pathway. Our results provide evidence that foraminiferal denitrification is
44 complemented by the foraminifera microbiome. The interaction of Foraminifera with their
45 resident bacteria is at the basis of foraminifera adaptation to anaerobic environments that
46 manifested in ecological success within oxygen depleted habitats.

47 **Introduction**

48 Nitrogen is an essential element for life on earth as it forms the basis for the synthesis of
49 nucleotides and amino acids. Nonetheless, while the earth atmosphere is rich in nitrogen gas
50 (up to 78%¹), this gas is usually inert but can be made accessible for biological processes by
51 nitrogen fixation². Microbial organisms are important players in the global nitrogen cycle as
52 they facilitate the assimilation of nitrogen into bioavailable nitrogen derivatives as well as the
53 dissimilation of nitrogen derivatives into dinitrogen (N₂)². A key dissimilatory pathway is
54 denitrification, where nitrate (NO₃⁻) is either partially or completely degraded and the final
55 product – N₂ – is released to the atmosphere (i.e., nitrogen loss)². Marine organisms are
56 considered major contributors to nitrogen loss from the environment with benthic organisms
57 being responsible for about two-thirds of the loss of reactive nitrogen in the ocean^{3,4}. Especially
58 oxygen minimum zones (OMZs) are worth mentioning here as they are estimated to be
59 responsible for 20-40% of bioavailable nitrogen removal in the ocean^{3,5}. The ability to perform
60 denitrification is abundantly found in eubacteria⁶, whereas it is rare among the eukaryotes.
61 Partial or complete denitrification have only been reported for two species of fungi⁷ and several
62 foraminifera of the order Rotaliida⁸⁻¹¹. Denitrifying foraminifera are unicellular eukaryotes
63 commonly found in marine sediments. Studies of foraminifera residing in the Peruvian OMZ

64 showed that they are found in high densities of up to 600 individuals per cm², where they are
65 estimated to contribute 20%-50% to the total benthic nitrate loss in the OMZ^{10,12}.

66 Rotaliid foraminifera are traditionally divided into three clades based on their
67 phylogeny¹³. Only species in clades I and III were demonstrated to denitrify, while rotaliids
68 classified in clade II have been shown to lack an intracellular nitrate storage or measurable
69 denitrification activity⁹. Class II rotaliids typically populate environments with poor-nitrate
70 supply, e.g. intertidal to near-shore habitats from the tropics up to boreal bioprovinces¹⁴, hence
71 it is conceivable that they lack the ability to denitrify. One example is *Ammonia tepida* (class
72 II), that can survive episodic oxygen depletion events via dormancy¹⁵. A study of clade III
73 species sampled from a hypoxic environment (Gulmarfjord, Sweden) – *Globobulimina* spp. –
74 showed that that their genome encodes several genes along the denitrification pathway that
75 are of ancient bacterial origin¹¹. These include the copper-containing nitrite reductase (NirK)
76 and nitric oxide reductase (Nor), but not the nitrate reductase (NapA/NarG) and nitrous oxide
77 reductase (NosZ). In addition, the *Globobulimina* genome contains a diverse gene family
78 encoding for nitrate transporters (Nrt)¹¹, a finding that is consistent with the accumulation of
79 an intracellular NO₃⁻ storage in denitrifying rotaliids^{8-10,16}. More recent studies could validate
80 the presence of those genes in at least two additional species of foraminifera and provide
81 alternative suggestions on the nitrate reductase homolog missing from the earlier model of
82 denitrification in foraminifera^{17,18}. The rotaliids ability to respire both oxygen (O₂) and NO₃⁻
83 marks them as facultative anaerobes that are able to thrive in both aerobic and anaerobic
84 conditions. Furthermore, while oxygen is generally considered to be preferred over NO₃⁻ as
85 electron acceptor, rotaliids from the Peruvian OMZ were reported to prefer NO₃⁻ over O₂¹⁰.
86 These findings suggest that genes of the denitrification pathway are widespread in rotaliids,
87 however their distribution remains largely unknown.

88 Foraminifera, like other eukaryotes¹⁹, are habitat to bacterial organisms that reside out-
89 and in-side their cell (i.e., test)²⁰⁻²⁴. Microscopic observations showed that the bacteria are
90 localized in food vacuoles or in the cytoplasm of the cell, which led to the suggestion that
91 interactions of foraminifera with its microbiota may vary from prey-predator interactions or
92 parasitism to metabolic symbiosis²². Further studies of the microbiota in clade II rotaliids
93 identified sulphate-reducing and sulphur-oxidizing bacteria that were suggested to participate
94 in Sulphur cycling thus providing carbon and other nutrients to the host^{20,21,25}. Notwithstanding,
95 previous studies of foraminifera-associated bacteria used microscopy observations or
96 sequencing of marker genes (e.g., 16S rRNA) that are limited in their resolution²⁰⁻²⁵. It has
97 been suggested that the microbiota of denitrifying foraminifera include denitrifying bacteria
98 that utilize the foraminifera NO₃⁻ storage, similarly to observations in other bacteria-protist
99 associations (e.g., Gromiids²⁶, allogromiids²⁷). Indeed, metagenomics of the *Globobulimina*

100 microbiota revealed the presence of a taxonomically diverse species community where
101 several members encode homologs of NapA and NosZ¹¹. This finding gave rise to the
102 hypothesis that the partial foraminiferal denitrification pathway may be complemented by
103 microbiota functions.

104 Here we investigate the evolutionary history of genes along the denitrification pathway
105 in foraminifera and furthermore examine the functional repertoire of the foraminifera
106 microbiome. For that purpose, we studied populations of ten rotaliid species known to
107 denitrify¹⁰ (except *Globobulimina pacifica* for which no information is available). Our study
108 supplies insights in the evolution of rotaliids and their microbiota and lays the basis for further
109 research of foraminifera genome evolution.

110

111 **Results**

112 **Transcriptomes of ten Peruvian rotaliids**

113 Eukaryotic transcriptomes and whole metagenomes were sequenced from populations of
114 foraminifera with two biological replicates per species (ca. 160 individuals per sample; see
115 sampled species in Figure 1A). Our computational analysis includes five additional publicly
116 available transcriptomes of foraminifera (Suppl. Table S1) and the genome data of one
117 monothalamid species (*Reticulomyxa filosa*). The assessment of transcriptome completeness
118 showed that ~90% of the eukaryotic marker proteins are present in the data of the ten newly
119 sequenced species. Furthermore, we examined the purity of the focal species in each
120 transcriptome by testing for an over-representation of eukaryotic marker proteins that are
121 expected as single-copy genes. A high redundancy of single-copy genes was found in the *B.*
122 *spissa* (78%) and *B. costata* (50%) transcriptomes, suggesting the presence of bystander
123 species in those samples (Suppl. Table S1).

124 **The Peruvian rotaliids harbour genes of the denitrification pathway**

125 To explore the denitrification mechanisms in the Peruvian foraminifera, we searched for
126 homologs to denitrification pathway genes. Our results reveal that all sampled species harbor
127 homologous genes to Nrt, NirK and Nor (Figure 1B; note that genes are termed by their
128 corresponding protein symbol). Our search for homologs in the publicly available data yielded
129 a putative homolog of NirK in *Rosalina* sp. and Nrt homologs in all but *R. filosa* (Fig. 1B). The
130 additional species we included here are considered to reside mostly in oxygenated habitats,
131 hence they are not expected to be able to perform denitrification. Among this group, only *A.*
132 *tepida* was so far experimentally tested for denitrification ability and reported as a non-
133 denitrifying species⁹. The reconstructed phylogenies of Nrt and NirK reveal two major sub-
134 clades where each clade includes most of the rotaliids in our study (Suppl. Figure S2; Suppl.

135 Table S2). This result indicates that Nrt and NirK underwent an ancient gene duplication where
 136 the two sub-clades encode for different subtypes of the proteins. Our results thus demonstrate
 137 that the denitrification pathway is highly conserved in the Peruvian rotaliids.
 138

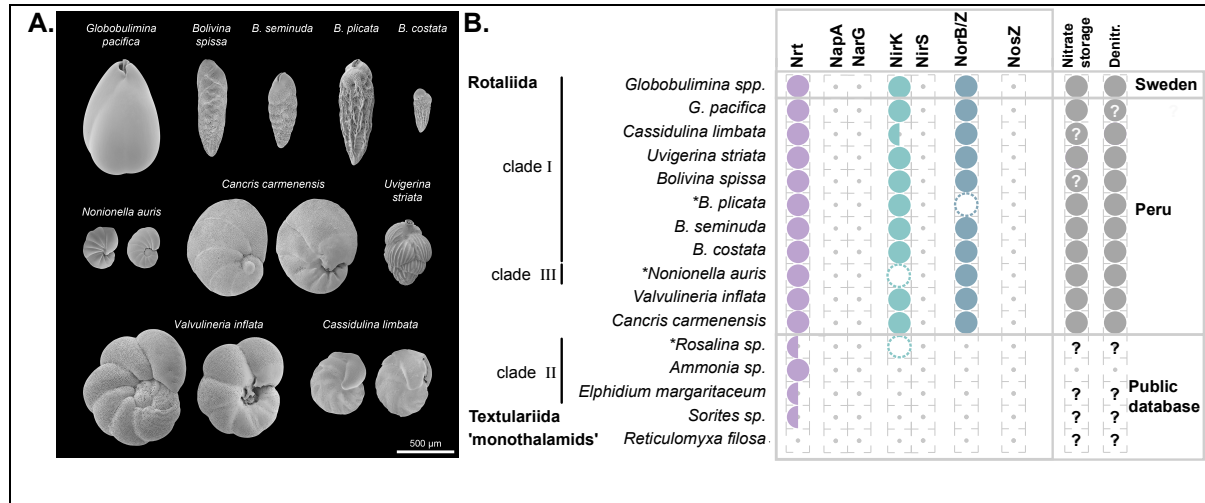


Figure 1. Morphological characteristics of the sampled Rotaliids and denitrification gene repertoire. A) Scanning electron micrographs of the sampled species. Species with clearly distinct lateral views are shown from two sides. **B)** Presence/absence of homologs of denitrification proteins identified for different foraminifera. Half circles indicate species where only a single, of multiple subtypes, was found. Dashed circles illustrate homologs discarded due to low coverage and asterisks highlight corresponding species. Evidence for NO₃⁻ storage and/or denitrification activity is illustrated by closed circles in the last column. Question marks denote missing information. Foraminifera sampled in this study are highlighted by the location 'Peru'. Protein symbols: Nrt: nitrate/nitrite transporter; NapA: periplasmic nitrate reductase; NarG: membrane-bound nitrate reductase; NirK: copper-containing nitrite reductase; NirS: cd₁-containing nitrite reductase; Nor: nitric oxide reductase; NosZ: nitrous oxide reductase. Note that the identification of homologous genes is based not only on sequence similarity but also on transcript abundance in order to exclude bystander species in the data. The additional data filtration stage affected our findings for *Rosalina* sp., *B. plicata* and *N. auris* (Suppl. Table S2 & S3), where the presence of at least one the crucial homologs (i.e. NirK or Nor) remained in the *B. plicata* and *N. auris* metatranscriptomes.

139

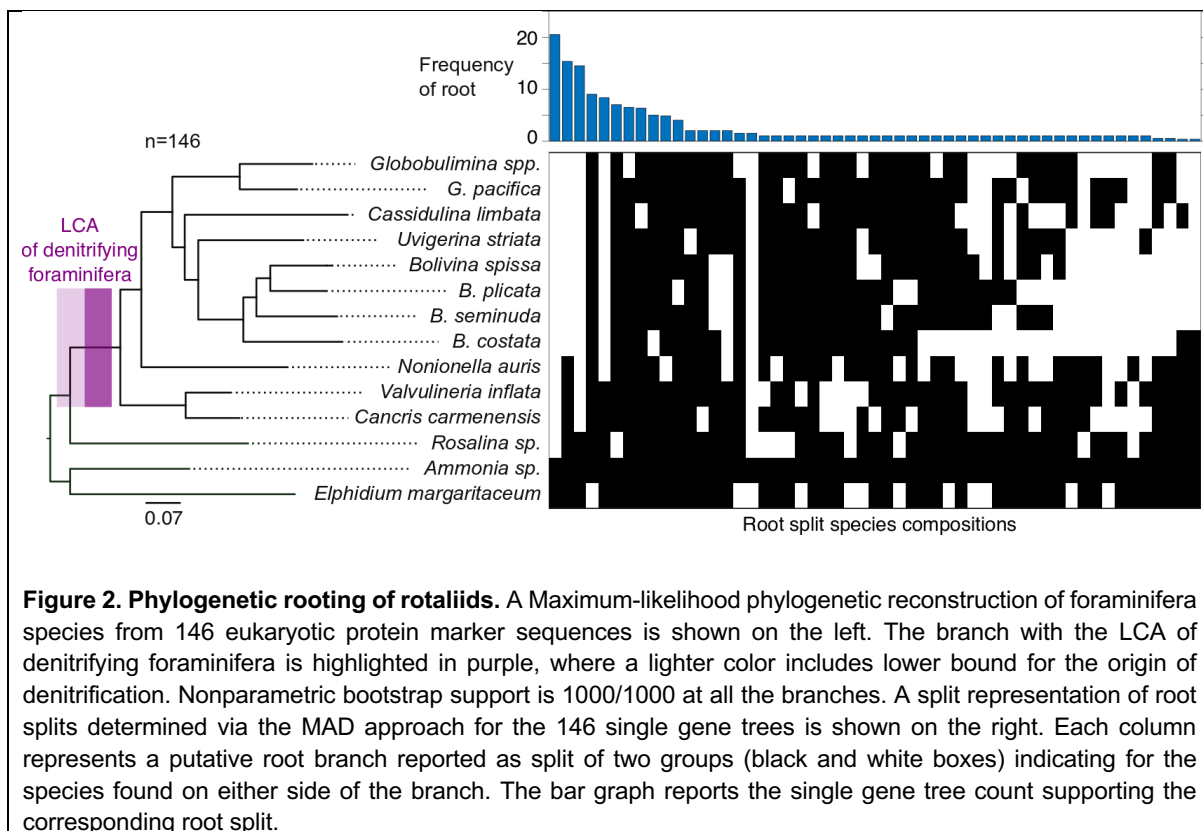
140 Foraminiferal denitrification evolved in the Rotaliida ancestor

141 The presence of NirK and Nor homologs the tested rotaliids suggests that those genes may
 142 have an ancient origin in this order. To study the origin of denitrification in foraminifera, we
 143 reconstructed the phylogenetic relations among species in our data using 81 eukaryotic
 144 marker proteins that have homologs in all species analyzed here (Suppl. Figure S1; Suppl.
 145 Table S4). Here, we applied a phylogenomics approach where the root position is inferred
 146 from all marker genes independent of a single species tree²⁸ (see methods). Our results show
 147 that the best-supported root position (42% of the gene trees) was at the branch leading to *R.*
 148 *filosa* (Suppl. Figure S1). This result is in agreement with previous studies that assumed
 149 monothalamids to be an outgroup in foraminifera phylogenies²⁹. The second most frequent
 150 root position was found at the branch leading to the miliolid *Sorites* sp. (15% of single gene
 151 trees), which was followed closely by a root position on the branch leading to *Rosalina* sp.

152 (12%). Taken together, the inferences of rooted topologies show that the Peruvian rotaliids,
153 together with *Globobulimina* spp. form a monophyletic group. Thus, our results reveal a shared
154 origin of denitrification in foraminifera and hence the evolution denitrifying foraminifera from
155 within the order Rotaliida.

156 For the inference of the denitrifying rotaliids last common ancestor (LCA; i.e., the
157 rotaliids root), we reconstructed phylogenetic trees from an extended set of 146 eukaryotic
158 marker proteins considering only members of the Rotaliida (Figure 2; Suppl. Table S4). An
159 examination of the rooted tree topologies revealed that the branch leading to *Ammonia* sp.
160 and *E. margaritaceum* was the most frequently supported root position (14% of single gene
161 trees). This root inference is further supported by an alternative root position at a branch that
162 splits *Ammonia* sp., *E. margaritaceum* and *Rosalina* sp. from the remaining species (10%).
163 Overall, the different alternative root positions support with 35% a Rotaliida LCA within clade
164 II foraminifera (i.e., among *Ammonia* sp., *E. margaritaceum* & *Rosalina* sp.; Fig. 2). The
165 absence of denitrification genes in clade II members (Fig. 1) further supports the suggestion
166 that the evolution of denitrification in rotaliids occurred by gene gain¹¹.

167

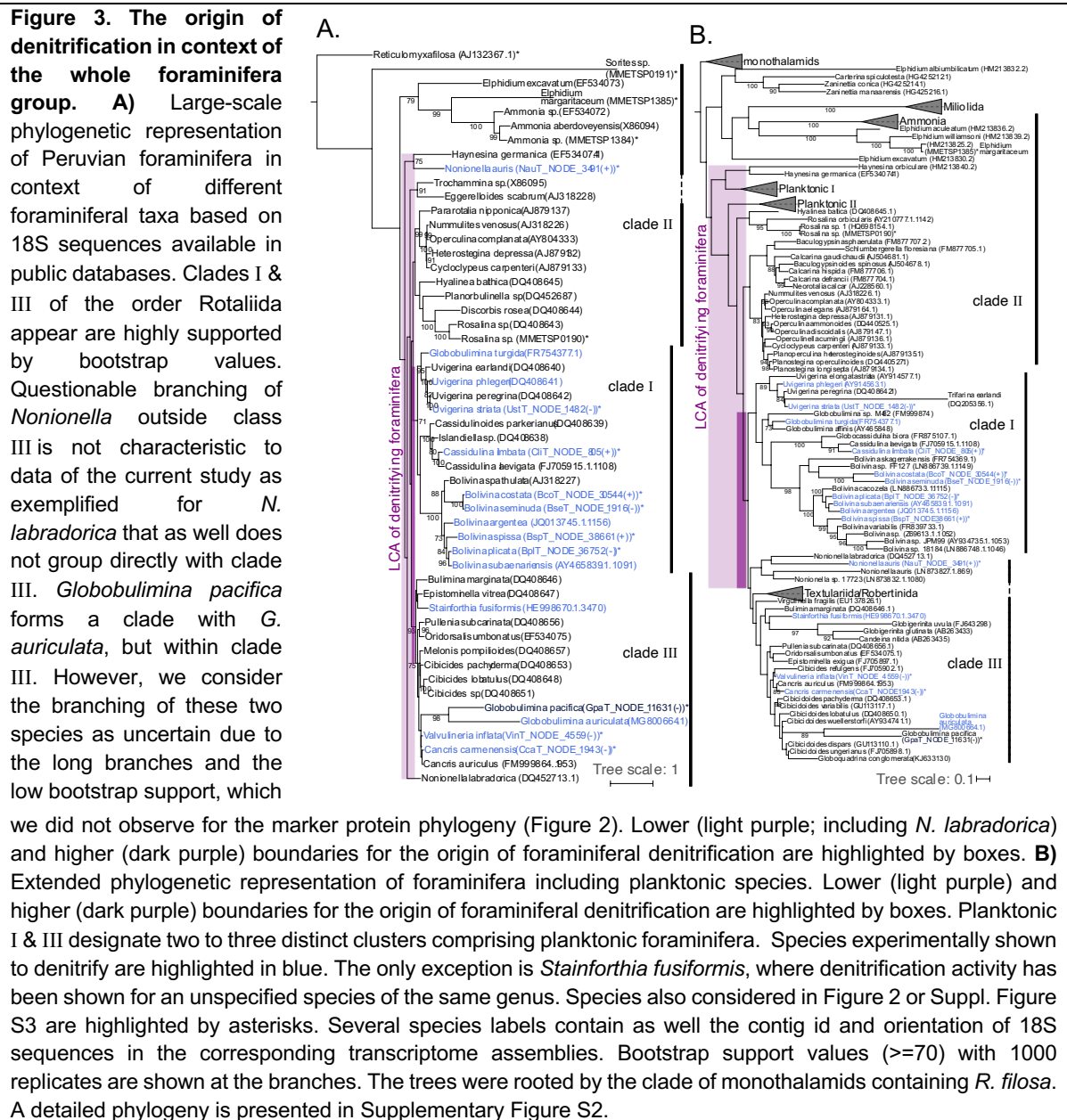


168

169 Ancient origin of denitrification in foraminifera

170 To further study the denitrifying foraminifera LCA, we examined the phylogenetic position of
171 the Peruvian species in the context of a foraminifera species tree. For that purpose, we

172 extracted sequences of the 18S ribosomal RNA (rRNA) subunit from our transcriptome data
 173 and used it in combination with publicly available 18S rRNA sequences to reconstruct a
 174 foraminifera species phylogeny (Figure 3A; Suppl. Table S5). The resulting rooted topology
 175 was mostly in agreement with the rotaliids phylogeny, where the focal species are found next
 176 to their closest relatives. Most species grouped well with their previously defined clades with
 177 the exception of *Nonionella* and *Globobulimina* representatives. Furthermore, several taxa
 178 were not monophyletic, as has been previously observed in foraminifera 18S rRNA
 179 phylogenies^{29,30}.



180

181 The inference of the denitrifying foraminifera LCA enabled us to further reconstruct the
 182 origin of denitrification within the foraminifera. For that purpose, we examined an extended
 183 phylogeny with additional foraminifera groups including planktonic species (Figure 3B; Suppl.

184 Figure S3). While the general taxonomic relationships in the tree were recovered as before
185 (i.e., Fig 3A), many branches had a low bootstrap support. For example, the rotaliid clades
186 II and III are paraphyletic, in contrast to the phylogeny with less taxa (Figure 3A). Nonetheless,
187 an LCA of clades I and III can be recovered. The previously unassigned genera *Valvulineria*
188 and *Cancris*⁹ grouped well with members of clade III in both 18S rRNA phylogenies, hence
189 they can be classified as clade III.

190 Since both clades I and III harbour several denitrifying foraminifera, it is most
191 parsimonious to conclude that LCA of clades I and III was likely a denitrifying organism. Our
192 inference thus suggests the presence of denitrification genes (and hence the capability) in all
193 members of clades I and III including e.g., the genera *Cibicoides* and *Virgulinema*, which were
194 previously not considered as denitrifying. Indeed, *Cibicoides wullerstoerfi* has been assumed
195 for a long time to be unable to withstand O₂ depletion³¹. However, recent studies observed
196 living *Cibicoides spp.* thriving in environments of < 2 µmol/kg O₂³² and fossil specimens in
197 the paleorecord during periods of severe O₂ depletion³³. These recent studies support our
198 prediction that several *Cibicoides spp.* are able to denitrify.

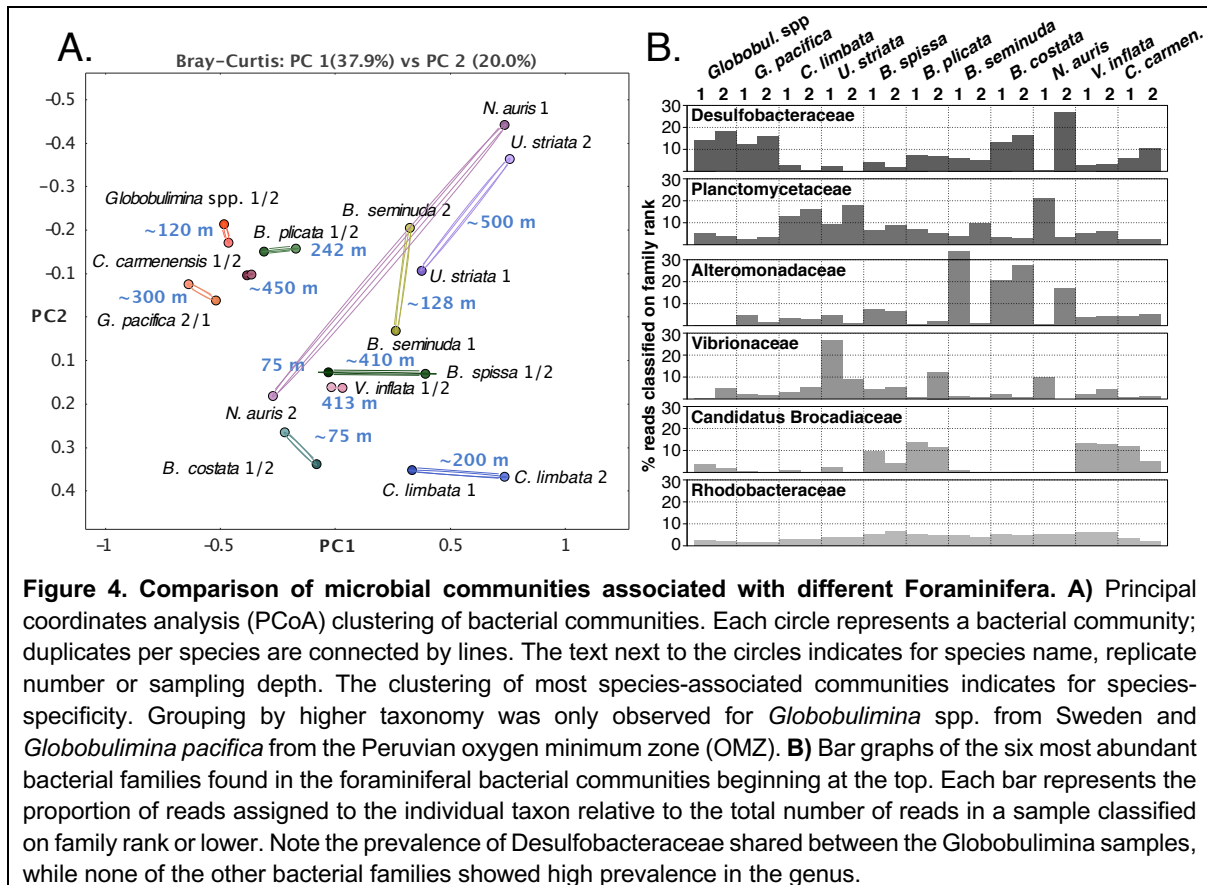
199

200 **Composition of the foraminifera microbiome is species-specific**

201 To test for bacterial contribution to the foraminifera denitrification, we examined the
202 foraminifera microbiome. For that purpose, we compared the composition of bacterial
203 communities among foraminifera in our sample. In the absence of species-specific interactions,
204 we would expect a strong impact of the environment (i.e., sampling location and water depth)
205 on the microbiome composition. Thus, we compared the microbial community composition
206 between foraminifera species and their sampling depths (Figure 4A). Our results show that
207 the individual microbiomes are clustered by the foraminifera species rather than the sampling
208 location, indicating the presence of species-specific bacterial communities in foraminifera. Our
209 results reveal a similar taxonomic composition of bacterial communities associated with
210 *Globobulimina spp.* from Sweden and *G. pacifica* from the Peruvian OMZ (Figure 4A). The
211 similarity in microbiome composition among the *Globobulimina* species indicates the presence
212 of genus-specific microbiome.

213 To identify common key players in foraminifera microbiota we examined the relative
214 abundance of all bacterial families in their microbiome (Figure 4B; Suppl. Table S6). Our
215 results revealed that the most prevalent bacterial families are Desulfobacteracea followed by
216 Planctomycetaceae. The relative abundance of these two families varied between different
217 species and samples. Furthermore, communities with a high relative abundance of
218 Desulfobacteracea are characterized by a low abundance of Planctomycetaceae and vice
219 versa ($r_s=-0.77$, p-value < 0.01, using Spearman correlation coefficient and t-test).

220 Desulfobacteraceae comprise sulphate-reducing bacteria and several representatives that are
 221 able to grow chemoautotrophically³⁴. Members of this group were previously observed in
 222 association with other rotaliids like *Virgulina fragilis* and members of clade II^{20,25}.
 223 Planctomycetes are often found in association with macroalgae³⁵; they are characterized by a
 224 diversified metabolism allowing them the of colonization of a wide range of habitats³⁵.
 225



226
 227 The next most abundant families were Alteromonadaceae, Vibrionaceae and
 228 `Candidatus Brocadiaceae` that were more diverse in their relative abundances across
 229 different species and replicates. Most reported `Candidatus Brocadiaceae` members are
 230 autotrophic, obligately anaerobic bacteria performing anammox, which is a dissimilatory
 231 pathway where ammonium and nitrite (NO₂⁻) are metabolized into N₂³⁶. The presence of nitrate
 232 storage in foraminifera and NirK suggest that nitrite is readily available inside the foraminifera
 233 test. Vibrionaceae are a diverse group including multiple species that colonize marine
 234 organisms either as symbionts^{37,38} or pathogens³⁹. Alteromonadaceae were isolated from
 235 diverse marine environments including eukaryotic microbiota⁴⁰. They are considered to be
 236 aerobe or facultative anaerobe bacteria and generally lack denitrification capabilities⁴¹. Finally,
 237 another abundant family, Rhodobacteraceae, is worth mentioning, as it is always found in low,
 238 but similar abundance in all samples. Marine Rhodobacteraceae species are considered

239 ecological generalists⁴²⁻⁴⁴ and have been reported to colonize marine animals (e.g., fish larvae
240 or sponges^{45,46}). The uniform distribution of Rhodobacteraceae in the foraminifera-microbiome
241 suggests that members of this group are permanent residents in the foraminifera microbiota.

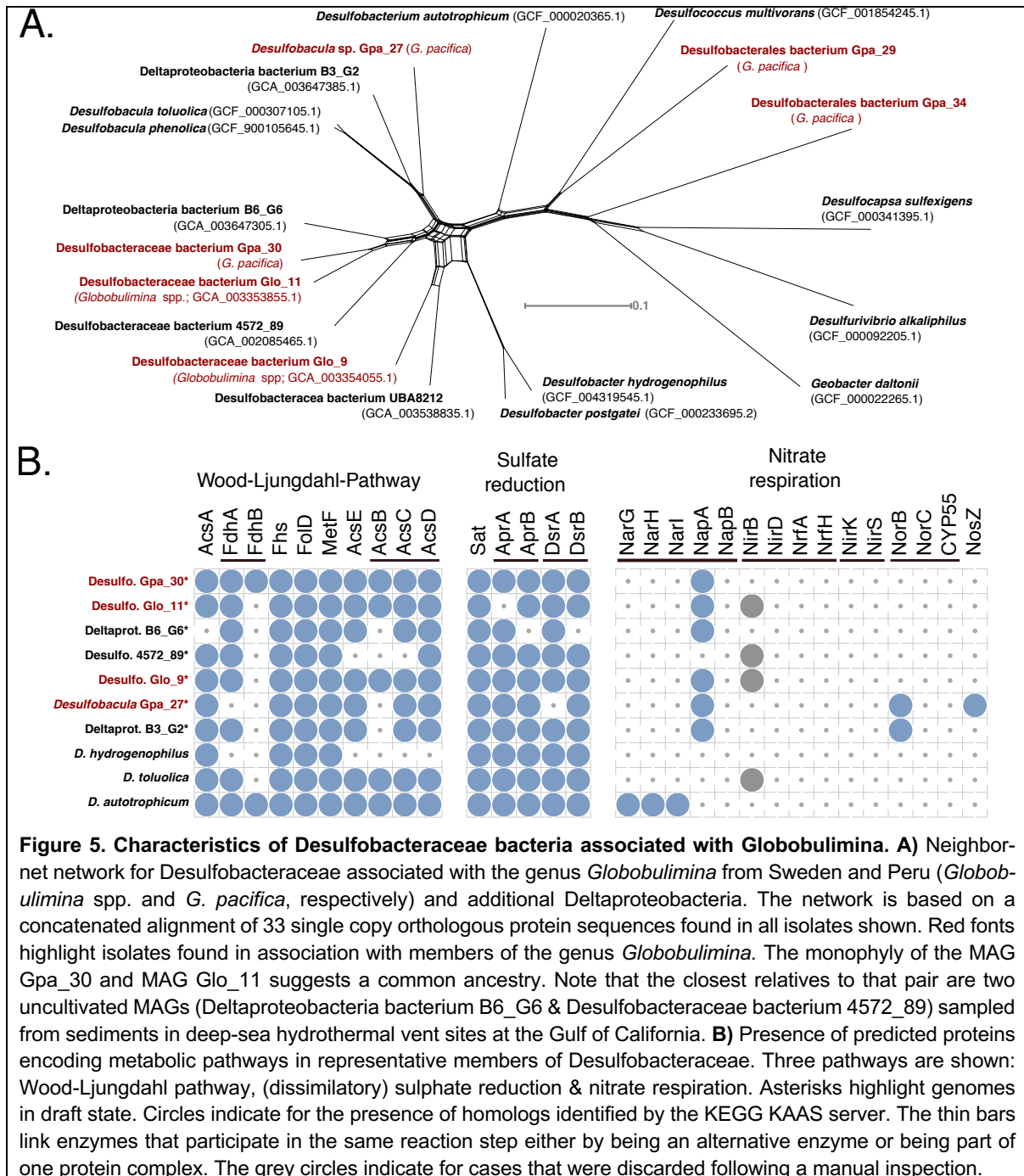
242 Our data thus shows that rotaliids are habitat to bacterial communities whose
243 composition is akin to the microbiota of other marine eukaryotes.

244 **An ancient interaction between Desulfobacteraceae and *Globobulimina* hints to** 245 **metabolic dependency**

246 The metagenomes analysis and classification into bacterial metagenome-assembled
247 genomes (MAGs) resulted in a total of 263 high-quality MAGs (i.e., draft bacterial genomes)
248 of foraminifera-associated bacteria (Suppl. Table S1). The strongest signal for a stable core
249 microbiome in our data was observed in the comparison among the *Globobulimina* species,
250 whose microbiome is characterized by a high frequency of Desulfobacteraceae (Figure 4B).
251 To further explore the association between *Globobulimina* and Desulfobacteraceae we
252 examined the Desulfobacteraceae MAGs in our data. A total of 40 high quality MAGs were
253 obtained from the *G. pacifica* metagenome, including four high quality draft MAGs classified
254 as Desulfobacteraceae. These were compared with the 26 previously published MAGs for
255 *Globobulimina* from Sweden, which include two Desulfobacteraceae MAGs¹¹ (Suppl. Table S7).
256 A phylogenetic network of the Desulfobacteraceae MAGs reveals two MAGs from the
257 *Globobulimina* spp. and *G. pacifica* metagenomes (Glo_11 & Gpa_30) that appear as sister
258 taxa. The average nucleotide identity (ANI) between both MAGs was 84%, which is within the
259 range expected for inter-species sequence similarity (e.g., within genera⁴⁷). The common
260 ancestry of these two MAGs suggests that the association between Desulfobacteraceae and
261 *Globobulimina* has an ancient origin. Our results thus indicate that the interaction fidelity
262 between *Globobulimina* and Desulfobacteraceae is high, similarly to observations in other
263 eukaryote-bacterial symbioses (e.g., oligochaete worms and sulfur bacteria⁴⁸ or marine
264 sponges with bacteria of the Poribacteria phylum⁴⁹).

265 A central foundation in the evolution of symbiotic interaction is an exchange of
266 currencies (i.e., resources) between the partners⁵⁰. The versatile metabolic capabilities of
267 Desulfobacteraceae and the availability of intracellular NO₃⁻ storage in foraminifera may
268 suggest that the interaction between Desulfobacteraceae and *Globobulimina* is based on
269 nutritional currencies. To further examine possible symbiotic interaction between
270 Desulfobacteraceae and *Globobulimina*, we searched for metabolic properties of the
271 Desulfobacteraceae MAGs that could serve as nutritional currencies in the symbiosis. For that
272 purpose, we surveyed the metabolic pathways of representative Desulfobacteraceae MAGs
273 with respect to carbon, sulfur and nitrogen metabolism (Figure 5B; Suppl. Table S8). Our
274 results reveal that all MAGs sampled encode the genetic repertoire required in order to

275 perform dissimilatory sulfate reduction as well as the Wood-Ljungdahl pathway. Anaerobic
 276 respiration via the dissimilatory sulfate reduction to sulfide is widespread among
 277 Desulfobacteraceae. Members of this family that encode the Wood-Ljungdahl pathway are
 278 able to oxidize organic compounds to carbon dioxide⁵¹. Alternatively, the Wood-Ljungdahl
 279 pathway may function in CO₂ carbon fixation during autotrophic growth.



280

281 Genes along the denitrification pathway (or NO₃⁻ respiration) are mostly absent from
 282 all Desulfobacteracea MAGs, except for periplasmic NO₃⁻ reductases (NapA) homologs that
 283 were found in most foraminifera-associated MAGs (for a review in NapA function see ⁵²). All

284 MAGs lack the typical NapB protein forming a complex with NapA. However, *nap* operons
285 without NapB genes have been reported for other members of Deltaproteobacteria, e.g.
286 *Desulfovibrio desulfuricans*⁵³. Notably, we found that the genome of *Desulfobulbus*
287 *propionicus* (Accession: GCA_000186885.1), a member of the order Desulfobacterales that
288 has been demonstrated to grow based on NO₃⁻⁵⁴, is lacking a gene for NapB. Hence NO₃⁻
289 respiration in Desulfobacterales in the absence of NapB is possible. We further hypothesize
290 that NapA may be secreted by the bacteria to *Globobulimina* intra-cellular environment. Indeed,
291 we found that the NapA sequences of all MAGs (and *D. desulfuricans*) include signal peptides
292 of the twin-arginine translocation pathway (reviewed in ⁵⁵) indicating that those proteins can
293 be translocated across cellular membranes. Our results suggest that the *Globobulimina*-
294 associated Desulfobacteraceae are able to reduce NO₃⁻ to NO₂⁻, and thus contribute to the
295 foraminiferal denitrification by performing the first reaction in the denitrification pathway for
296 which we found no evidence in the foraminifera transcriptomes.

297 **Discussion**

298 Our results demonstrate that foraminifera are habitat to bacterial communities that may play
299 a role in their ability to thrive in oxygen-depleted habitats. A recent study demonstrates the
300 endosymbiotic contribution to denitrification within a ciliate host⁵⁶. However, previous studies
301 of denitrification in foraminifera argued against the possibility of bacterial contribution to
302 foraminiferal denitrification^{8,11}. Notably, most species in the foraminifera microbiota are
303 considered strict anaerobes, hence, when exposed to oxygen the foraminifera may lose their
304 associated microbiota. Metagenomics sequencing of samples frozen directly after sampling is
305 thus an important source of information on the composition and function of the foraminifera
306 microbiome.

307 Our results indicate that Desulfobacteracea members of the foraminifera microbiota
308 can utilize the NO₃⁻ storage accumulated by their host. Whether the NO₃⁻ reduction by bacteria
309 is beneficial to the foraminifera remains, however, an open question. The bacteria may use
310 the NO₃⁻ it for their own respiratory processes or to build up organic compounds via the
311 assimilation of NO₃⁻. For example, it has been suggested that a proportion of NO₃⁻ taken up
312 by the foraminifera *Ammonia beccari* was used for amino acid synthesis, probably by resident
313 bacteria²¹. Previously we speculated about a foraminiferal sulfite reductase homolog
314 performing the conversion of NO₃⁻¹¹. Yet, considering the absence of foraminifera homologs
315 to NO₃⁻ reductase and the presence of NapA in all sampled Desulfobacteraceae MAGs, it is
316 tenable to hypothesize that the reduction of NO₃⁻ to NO₂⁻ in foraminifera is performed by
317 resident bacteria.

318 An association between foraminifera and Desulfobacteracea has been previously
319 reported. For example, the presence of a putative Deltaproteobacterium (Desulfobacteracea)
320 was previously described for *Virgulinema fragilis*²⁰, a foraminifera that we here predict to be a
321 denitrifying species (Figure 3B). Furthermore, foraminifera from the genera *Ammonia*,
322 *Elphidium* and *Haynesina* that are not expected to denitrify were found to harbor members of
323 Desulfobacterales bacteria²⁵. Hence, the interaction between foraminifera and
324 Desulfobacteracea may involve alternative nutritional currencies. Previous studies refer to the
325 role of Desulfobacteracea in sulphur cycling and carbon/nutrient acquisition^{20,21,25}. Especially
326 the carbon fixation capabilities via Wood-Ljungdahl pathway would be highly beneficial for the
327 heterotrophic lifestyle of foraminifera, similarly to other symbioses that involve fixed-carbon as
328 a nutritional currency (e.g., as in deep-sea mussels⁵⁷ or sponges⁴⁹).

329 The radiation of early foraminifera species has been estimated to occur between 690
330 and 1,150 million years ago (mya), while the first primitive rotaliids appeared in the late
331 Permian around 260 mya^{58,59}. Most of the rotaliids superfamilies diverged in the mid to late
332 Triassic between approximately 240 and 200 mya^{29,60,61} and the majority of extant species
333 diverged during the Miocene (23.8 - 5.5 mya⁶²). Our phylogenetic analyses suggest that clades
334 I and III diversified from within clade II, while the LCA of clade I probably originated from
335 within clade III (Figures 2 & 3). Although most species reported to denitrify were reported from
336 the Peruvian OMZ and Sweden, representatives of corresponding genera are found all over
337 the world (Suppl. Table S5). Therefore, most extant rotaliids likely diversified from a
338 denitrifying LCA far back in time. The origin of foraminiferal denitrification within or after
339 diversification from members of clade II may coincide with the rapid increase of fossil records
340 at the onset of the late Cretaceous ~100 mya^{60,61}. Our results therefore indicate that eukaryotic
341 denitrification by rotaliids emerged late in foraminiferal evolution, possibly during the
342 worldwide Cretaceous Ocean Anoxic Events^{63,64}.

343 Considering the high conservation of nitrate transporters (Figure 1) and the
344 observation of nitrate storage in many divergent species⁹, it is tenable to speculate that
345 foraminifera had the mechanisms for nitrate import and storage long before they evolved the
346 ability to denitrify. NO₃⁻ transporters are ancient eukaryotic enzymes that play a role in the
347 NO₃⁻ assimilation machinery and they are encoded in genomes of photoautotrophs such as
348 plants and saprotrophs like fungi^{65,66}. In contrast to bacteria, foraminifera (as most
349 heterotrophs) are unable to perform NO₃⁻ assimilation on their own. Thus, NO₃⁻ accumulated
350 by the foraminiferal hosts could have fuelled bacterial NO₃⁻ metabolism of associated bacteria
351 in exchange for organic compounds. We propose that denitrification by symbiotic bacteria was
352 indeed the ancestral state of denitrification in foraminifera, similarly to gromiids²⁶, which share
353 a common evolutionary origin with foraminifera⁶⁷. The finding of bacterial-like denitrification

354 genes in rotaliids furthermore suggests that foraminifera may have acquired those genes from
355 bacteria¹¹. Thus, a rare gene acquisition from a foraminifera-associated, denitrifying bacterium
356 could have been at the origins of foraminiferal (eukaryotic) denitrification. Notably, the rotaliids
357 denitrification gene set is incomplete and it varies among the species sampled here (i.e., *N.*
358 *auris*, *B.plicata* or even *Rosalina* sp.). Species reported to release N₂O instead of N₂⁹ further
359 support our observation. Thus, the presence of a partial denitrification pathway in rotaliids as
360 well as in their resident Desulfobacteracea may suggest that the acquisition of denitrification
361 ability in foraminifera occurred in multiple stages and is not yet complete.

362

363 **Methods**

364 **Foraminifera sampling**

365 Samples were collected off the Peruvian coast in the 2017 Austral winter (R/V Meteor M137)
366 as described by Glock et al. 2019¹⁰. Briefly, sediment samples were taken with a video-guided
367 sediment multiple corer (MUC) containing 6 liners along a depth transect at 12°S. The top 1
368 to 3 cm of the sediment cores were sampled and immediately wet sieved with surface water
369 through stacked sieves with mesh size of 2000µm to 63µm to retrieve benthic foraminifera. The
370 foraminifera were rinsed in sterile seawater obtained by filtering core-overlying seawater with
371 a sterile bottle top filtration system (Durapore filter, 0.2 µm) and a vacuum pump within 40
372 minutes of MUC arrival on deck. Focal species were manually picked using a
373 stereomicroscope. These were characterised morphologically according to the literature⁶⁸⁻⁷⁰.
374 Up to 160 individuals (classified into focal species) were pooled in one cryo vial (2ml, RNase
375 free) and flash frozen in liquid nitrogen.

376 **Microscopy**

377 Individual foraminifera were dehydrated in a graded ethanol series (70 %, 80 %, 90 %, 96 %
378 and two times 100 %; 15 min each), air-dried for 12 h in a desiccator and mounted on
379 aluminium stubs (PLANO GmbH) using conductive and adhesive carbon pads (PLANO
380 GmbH). Subsequently, the preparations were sputter-coated with a 10-nm-thick gold-
381 palladium (80/20) layer using a high vacuum sputter coater Leica EM SCD500 (Leica
382 Microsystems GmbH) and visualised with a Hitachi S-4800 field emission scanning electron
383 microscope (Hitachi High-Technologies Corporation) at an acceleration voltages of 3 kV and
384 an emission current of 10 mA applying a combination of the upper detector and the lower
385 detector.

386 **Nucleic acid extraction, and sequencing**

387 Genomic DNA and total RNA from different biological samples were extracted using either the
388 DNeasy® Plant Mini kit (QIAGEN) for genomics (DNA) or simultaneously purified using
389 InnuPREP DNA/RNA Mini Kit (analytikjena) for transcriptomics (RNA). Foraminifera cells in
390 each samples (ca. 160 individuals) were disrupted by pestle-crashing on ice after immersion
391 of the containing cryo-vial in liquid nitrogen. Samples for genomics were treated with lysozyme
392 (200µl of 10mg/ml TE) and proteinase K (1mg/100µl). Samples for transcriptomics samples
393 were treated only with lysozyme (6 ul of 20mg/ml TE) before additional crashing and 2-minute
394 incubation was performed. After disruption and initial lysis, manufacturer protocols for the
395 respective nucleic acid extraction were followed with modifications to the elution volumes (2 x
396 50µl for DNA and 2 x 25µl for RNA). Libraries for genomics were produced after DNA
397 fragmentation (Covaris target 400, intensity 5, duty cycle 5% cycles per burst 200, 55sec
398 treatment time) using NEBNext® Ultra II DNA Library Prep Kit for Illumina®. Whereas,
399 transcriptomic libraries were produced using NEBNext® Ultra RNA Library Prep Kit for
400 Illumina® (NEB) with mRNA isolation performed with poly-A mRNA beads. All libraries were
401 produced in duplicates from two different sets of pooled individuals for each species and were
402 produced without protocol interruption. Before sequencing, each library was quantified with a
403 Qubit® fluorometer (Invitrogen by Life Technologies™) and qualified using a TapeStation
404 (Agilent technology). The libraries were sequenced paired-end (2 x 150 bp) on an Illumina®
405 HiSeq 4000 platform.

406

407 **Sequencing datasets of foraminifera**

408 Sequencing resulted in 4.6 billion paired-end reads covering 1.4 tera bases in total. This
409 includes transcriptome and metagenome datasets (BioProject accessions PRJNA494828 &
410 PRJNA503328). Reads were quality-checked by FastQC ver. 0.11.5
411 (<http://www.bioinformatics.babraham.ac.uk/projects/fastqc>; Aug 2016). Filtering and trimming
412 of reads was performed using Trimmomatic⁷¹ ver. 0.36 (Parameters:
413 ILLUMINACLIP:primers.fa:2:30:10 LEADING:5 TRAILING:5 SLIDINGWINDOW:4:5
414 MINLEN:21; the file 'primers.fa' contained adaptor and contaminant sequences provided by
415 Trimmomatic and FastQC). Processed reads from transcriptomes of the two samples per
416 species were assembled into transcript contigs using SPAdes⁷² ver. 3.11.1 ("--rna" option).
417 Protein sequences were translated from transcripts as the longest open reading frame (ORF)
418 using TransDecoder⁷³ ver. v5.0.2 ("-m 30" option). Final protein names consist of the contig
419 ids followed by the sequence positions covered by the CDS and an indicator for the forwards
420 (+) or reverse (-) strand. Transcript abundance of individual transcriptome datasets are
421 referring to Transcripts Per Million (TPM) determined by the Trinity pipeline⁷³ 2.4.0 (Trinity
422 script 'align_and_estimate_abundance.pl') via RSEM⁷⁴ ver. 1.2.30 and Bowtie⁷⁵ 2.1.0 using

423 paired-end reads. Additional raw sequencing reads were obtained from the Marine Microbial
424 Transcriptome Project (MMETSP; SRA accessions: *Rosalina* sp., SRR1296887; *Sorites* sp.,
425 SRR1296734; *Ammonia* sp., SRR1300434; *Elphidium margaritaceum*, SRR1300475) and
426 processed as described above. We found that the assembly obtained for *Sorites* sp. contained
427 a high proportion of sequences likely originating from an algal species (Probably
428 *Symbiodinium* sp.), which was removed by applying a binning approach considering only
429 contigs with GC-content $\leq 38\%$. Finally, we included data for *Globobulimina* spp. sampled in
430 Sweden from our previous study (Transcriptome data: GloT15¹¹) and proteins annotated on
431 the genome assembly of *Reticulomyxa filosa* (NCBI accession: GCA_000512085.1).

432

433 **Species phylogenies and rooting**

434 Transcriptome completeness and heterogeneity was determined by assessing genome
435 completeness via Benchmarking Universal Single-Copy Orthologs⁷⁶ (BUSCO v3; lineage
436 'eukaryota') method. Orthologous proteins determined as Complete (or Duplicated) by the
437 BUSCO analysis were merged into protein clusters to study phylogenetic relationships among
438 the species. In case of duplicated BUSCOs in metatranscriptomes, one representative was
439 inferred based on sequence similarity. Therefore, all orthologs retrieved for the same
440 metatranscriptome were compared to all members of the BUSCO protein cluster by global
441 pairwise alignments using needle (EMBOSS tools version 6.6.0⁷⁷). The ortholog with the
442 highest median sequence similarity over all comparisons was picked as the representative
443 sequence. Multiple sequence alignments used in the current study were obtained using
444 MAFFT⁷⁸ (Version: 7; parameter: 'linsi') and the phylogenetic trees were reconstructed using
445 IQTREE⁷⁹ (Version: 1.5.5 or 1.6.9; default parameters; note that ModelFinder is enabled by
446 default). Phylogenies were reconstructed for the individual BUSCO clusters. Due to their
447 morphological differences from other foraminifera groups, monothalamids like *R. filosa* have
448 been previously used as an outgroup for phylogenetic studies of foraminifera²⁹. Since the
449 choice of a distantly related outgroup may lead to erroneous rooted topology due to long
450 branch attraction⁸⁰, we further tested the robustness of the root position independent from
451 outgroup species. Root positions were determined using MAD²⁸ (Parameters: '-bsnn'). The
452 support in each root splits is calculated as the proportion of gene trees where the root position
453 was inferred as such²⁸. For the overall species trees, multigene phylogenies were
454 reconstructed using IQTREE (parameter: '-spp') considering all protein cluster alignments of
455 either foraminifera or Rotaliida.

456 Reference 18S rRNA sequences used for the large-scale phylogenies (Suppl. Table
457 S5) were obtained from NCBI, MMETSP, SILVA⁸¹, the foram barcoding project
458 (<http://forambarcoding.unige.ch/>) and the Planktonic Foraminifera Ribosomal Reference
459 database⁸² (PFR²). These sequences were used as database sequences to identify 18S

460 sequences from Peruvian species transcriptomes based on BLAST⁸³ (version: 2.2.28+;
461 options: '-task blastn -evaluate 1e⁻¹⁰') searches. Among the hits retrieved we searched for a
462 single representative transcript contig per transcriptome assembly. The transcripts with the
463 highest product of sequence length and sequencing depth (i.e., coverage given by SPAdes)
464 were determined as representative sequences for most of the focal species. However, for *B.*
465 *costata*, *V. inflata*, *G. pacifica* and *N. auris* different representative sequences were chosen
466 by giving sequence information (i.e., longer sequences) a higher weight than sequencing
467 depth. To obtain 18S phylogenies first the reference sequences were aligned with MAFFT and
468 subsequently representatives 18S rRNA sequences of the Peruvian transcriptomes were
469 added (MAFFT options: '--addfragments --adjustdirection') to the alignment followed by the
470 tree reconstruction using IQTREE.

471

472 **Identification of foraminiferal denitrification proteins**

473 To identify homologs to enzymes in the denitrification pathway, we used a similar approach
474 as previously established in Woehle et al. 2018¹¹ using the corresponding protein database
475 expanded by the protein sequences identified for *Globobulimina*¹¹. The search for
476 denitrification enzymes homologs in the transcriptome assemblies was performed with
477 BLASTP (parameter: '-max_target_seqs 1000000 e-value 1e-5'). Protein sequences of hits
478 with query coverage $\geq 40\%$ and sequence identity $\geq 20\%$ were extracted to obtain a first set
479 of homologs. We further applied a cutoff to discard lowly represented transcripts with TPM <
480 2 in at least one of the two replicates sequenced. With the resulting protein set, we reiterated
481 searches in the non-redundant NCBI protein (NR; version May 2018) and the RefSeq 88
482 database⁸⁴ using diamond v0.9.22 applying the '--more-sensitive' option. First best hit
483 sequences per query were obtained and clustered with CD-HIT 4.6⁸⁵ (option: "-c 0.98") to
484 reduce sequence redundancy. All obtained protein sequences of a given enzyme were aligned
485 with MAFFT and phylogenetic trees were reconstructed with IQTREE (parameters: '-bb 1000
486 -alrt 1000'). The trees were rooted using an outgroup, if available, or MAD.

487

488 **Metagenomics processing**

489 For the visualisation of metagenomic composition, trimmed paired-end reads from Peruvian
490 species samples and the *Globobulimina* 'Ambient' samples¹¹ were subsampled via BMap
491 (version 36.84; <https://sourceforge.net/projects/bbmap/>; 'reformat.sh' script; parameters:
492 'samplereadtarget=10000000 addslash=t'). The resulting reads were mapped against the NR
493 database with ac-diamond⁸⁶) and classified using MEGAN6⁸⁷ (Version 6.15.0; options '-a2t
494 prot_acc2tax-Nov2018X1.abin -a2eggnog acc2eggnog-Oct2016X.abin -a2seed acc2seed-
495 May2015XX.abin'). MEGAN6 was used for assessment of metagenomics communities and
496 visual representation (See Figure 4) that were classified up to the order rank level with different

497 taxon sets (e.g., all nodes or only the bacterial subtree). Metagenome assemblies were
498 obtained by combining all trimmed reads per focal species using MEGAHIT⁸⁸ (Version 1.1.3;
499 default settings). Individual bacterial genomes were obtained using the binning approach
500 implemented with MaxBin2⁸⁹ (Version 2.2.4; parameter: '-min_contig_length 500') using
501 coverage information of the two samples per species of foraminifera. Binning statistics were
502 assessed using CheckM⁹⁰ (Version 1.0.11); a threshold for completeness of at least 80% and
503 contamination of maximum 20% was applied to classify bacterial bins as draft genomes. The
504 protein sequences obtained via checkM were used for further classifications. The average
505 nucleotide identity (ANI) was calculated using a perl script obtained from
506 <https://github.com/chjp>.

507 For the taxonomic assignment of genome bins, we used the diamond tool to find first
508 best hits for each protein of a genome bin against the NR database (option: '-k 10'; e-value \leq
509 1e-10) and retrieved the corresponding taxonomic assignments (as we previously
510 described¹¹). For each bin, identical taxonomic hierarchies were counted with the genus being
511 the lowest rank considered, sorted accordingly and stepwise searched for the lowest
512 taxonomic rank supporting >50% of protein bin hits starting with the most abundant taxonomy.
513 'Environmental samples' and 'Cellular organisms' were not considered. For the phylogenetic
514 reconstruction of Desulfobacteracea we determined protein families as protein clusters using
515 sequences of Desulfobacteracea bins associated with *Globobulimina* and additional
516 Desulfobacteracea genomes downloaded from NCBI. First, we determined reciprocal best
517 BLAST hit pairs (rBBH; parameter: '-evaluate 1e-5') between all the Desulfobacteracea protein-
518 coding sequences⁹¹. Then rBBH pairs were globally aligned with the needle tool and pairs with
519 $\geq 30\%$ identical amino acids were sorted into clusters using the Markov clustering algorithm⁹²
520 (MCL; version 12-135). The 33 resulting protein clusters that contained a single copy for each
521 of the Desulfobacteraceae strains (i.e., universal single-copy clusters) were aligned with
522 MAFFT. The resulting alignments were concatenated and a splits network was reconstructed
523 with SplitsTree⁹³ (version 4.15.1). Prediction of protein function for bacterial genomes were
524 obtained using the KEGG Automatic Annotation Server⁹⁴ (KAAS; BBH method via BLAST and
525 the following species set: hsa, dme, ath, sce, pfa, eco, sty, hin, pae, nme, hpy, rpr, mlo, bsu,
526 sau, lla, spn, cac, mge, mtu, ctr, bbu, syn, aae, mja, afu, pho, ape, geo, dvu, dat, dpr, dol, dal,
527 dak, dps, drt, dba, dao, dbr). Global pairwise identities for NapA protein sequences were
528 inferred with needle. Signal peptides were predicted using the SignalP-5.0 webservice for
529 gram-negative bacteria⁹⁵.

530

531 **Data availability**

532 Sequencing reads are deposited at the single read archive (SRA) accessions SRR8144071
533 to SRR8144090 and SRR7971179 to SRR7971198. The assemblies are available at the

534 transcriptome sequencing archive (TSA; See Suppl. Table 1 for accessions) and as whole
535 genome shotgun (WGS) projects (See Suppl. Table 7 for accessions). All other information
536 on accessing data analysed in this study is included in the manuscript or in the supplemental
537 information.

538

539 **Acknowledgments**

540 We thank Devani Romero Picazo and Anne Kupczok for critical comments on the manuscript.
541 We gratefully acknowledge the scientific party and crew of the R/V Meteor cruise M137 as
542 well as Asmus Petersen and Matthias Türk for their support at sea. Samples from Peru were
543 obtained according to Peruvian access and benefit sharing regulations. We thank the Nagoya
544 officer of Kiel University - Dr. Scarlett Sett - for her support of our research. We further thank
545 Natalia Bernabe Lopez for her assistance in collecting metadata for the 18S sequences.
546 Genome sequencing was performed in the Centre for Genome Analysis Kiel that is funded by
547 the German Research Foundation (DFG). The study was supported by the Deutsche
548 Forschungsgemeinschaft (DFG) via the SFB 754 on Climate–Biogeochemistry Interactions in
549 the Tropical Ocean, the cluster of excellence The Future Ocean, and the European Research
550 Council (Grant No. 281357 awarded to TD). C.W. was supported by the Kiel Life Science (KLS)
551 Young Scientist Programme and would like to thank the Max Planck-Genome-centre Cologne
552 for their support in data analysis.

553 **Author contributions**

554 C.W., A.-S.R., N.G., T.W., J.W., D.R., J.S. & T.D. designed the research strategy and
555 performed sampling. C.W. analysed the transcriptomes and metagenomes. A.-S.R. performed
556 the experimental lab work. C.H. constructed incubation chambers. J.M. and S.N.G. produced
557 micrographs. C.W. and T.D. wrote the manuscript with input from all co-authors.

558

559 **Declaration of Interests**

560 The authors declare no competing interests.

561

562 **References:**

- 563 1. Cox, A. N. *Allen's Astrophysical Quantities*. (Springer, 2015). doi:10.1007/978-1-4612-
564 1186-0
- 565 2. Thamdrup, B. New Pathways and Processes in the Global Nitrogen Cycle. *Annu. Rev.*
566 *Ecol. Evol. Syst.* **43**, 407–428 (2012).

- 567 3. Gruber, N. in *The Ocean Carbon Cycle and Climate* **35**, 97–148 (Springer, Dordrecht,
568 2004).
- 569 4. Gruber, N. & Galloway, J. N. An Earth-system perspective of the global nitrogen
570 cycle. *Nature* **451**, 293–296 (2008).
- 571 5. Lam, P. *et al.* Revising the nitrogen cycle in the Peruvian oxygen minimum zone. *Proc*
572 *Natl Acad Sci USA* **106**, 4752–4757 (2009).
- 573 6. Philippot, L. Denitrifying genes in bacterial and Archaeal genomes. *Biochim. Biophys.*
574 *Acta* **1577**, 355–376 (2002).
- 575 7. Shoun, H., Kim, D. H., Uchiyama, H. & Sugiyama, J. Denitrification by fungi. *FEMS*
576 *Microbiology Letters* **73**, 277–281 (1992).
- 577 8. Risgaard-Petersen, N. *et al.* Evidence for complete denitrification in a benthic
578 foraminifer. *Nature* **443**, 93–96 (2006).
- 579 9. Piña-Ochoa, E. *et al.* Widespread occurrence of nitrate storage and denitrification
580 among Foraminifera and Gromiida. *Proc Natl Acad Sci USA* **107**, 1148–1153 (2010).
- 581 10. Glock, N. *et al.* Metabolic preference of nitrate over oxygen as an electron acceptor in
582 foraminifera from the Peruvian oxygen minimum zone. *Proc Natl Acad Sci USA* **116**,
583 2860–2865 (2019).
- 584 11. Woehle, C. *et al.* A Novel Eukaryotic Denitrification Pathway in Foraminifera. *Curr Biol*
585 **28**, 2536–2543.e5 (2018).
- 586 12. Glock, N. *et al.* The role of benthic foraminifera in the benthic nitrogen cycle of the
587 Peruvian oxygen minimum zone. *Biogeosciences* **10**, 4767–4783 (2013).
- 588 13. Schweizer, M., Pawlowski, J., Kouwenhoven, T. J., Guiard, J. & van der Zwaan, B.
589 Molecular phylogeny of Rotaliida (Foraminifera) based on complete small subunit
590 rDNA sequences. *Marine Micropaleontology* **66**, 233–246 (2008).
- 591 14. Murray, J. W. *Ecology and applications of benthic foraminifera*. (Cambridge University
592 Press, 2006).
- 593 15. LeKieffre, C. *et al.* Surviving anoxia in marine sediments: The metabolic response of
594 ubiquitous benthic foraminifera (*Ammonia tepida*). *PLoS One* **12**, e0177604 (2017).
- 595 16. Bernhard, J. M. *et al.* Potential importance of physiologically diverse benthic
596 foraminifera in sedimentary nitrate storage and respiration. *J Geophys Res* **117**,
597 G03002 (2012).
- 598 17. Gomaa, F. *et al.* Multiple integrated metabolic strategies allow foraminiferan protists to
599 thrive in anoxic marine sediments. *Sci Adv* **7**, (2021).
- 600 18. Orsi, W. D. *et al.* Anaerobic metabolism of Foraminifera thriving below the seafloor.
601 *ISME J* **14**, 2580–2594 (2020).
- 602 19. Zilber Rosenberg, I. & Rosenberg, E. Role of microorganisms in the evolution of
603 animals and plants: the hologenome theory of evolution. *FEMS Microbiology Reviews*
604 **32**, 723–735 (2008).
- 605 20. Tsuchiya, M. *et al.* Cytologic and genetic characteristics of endobiotic bacteria and
606 kleptoplasts of *Virgulinema fragilis* (Foraminifera). *J Eukaryotic Microbiology* **62**, 454–
607 469 (2015).
- 608 21. Nomaki, H. *et al.* Nitrate uptake by foraminifera and use in conjunction with
609 endobionts under anoxic conditions. *Limnology and Oceanography* **59**, 1879–1888
610 (2014).
- 611 22. Bernhard, J. M., Martin, J. B. & Rathburn, A. E. Combined carbonate carbon isotopic
612 and cellular ultrastructural studies of individual benthic foraminifera: 2. Toward an
613 understanding of apparent disequilibrium in hydrocarbon seeps. *Paleoceanography*
614 **25**, PA4206 (2010).
- 615 23. Bernhard, J. M., Habura, A. & Bowser, S. S. An endobiont-bearing allogromiid from
616 the Santa Barbara Basin: Implications for the early diversification of foraminifera. *J*
617 *Geophys Res* **111**, 399 (2006).
- 618 24. Bernhard, J. M. Potential symbionts in bathyal foraminifera. *Science* **299**, 861–861
619 (2003).
- 620 25. Salonen, I. S., Chronopoulou, P. M., Bird, C., Reichart, G. J. & Koho, K. A.
621 Enrichment of intracellular sulphur cycle –associated bacteria in intertidal benthic

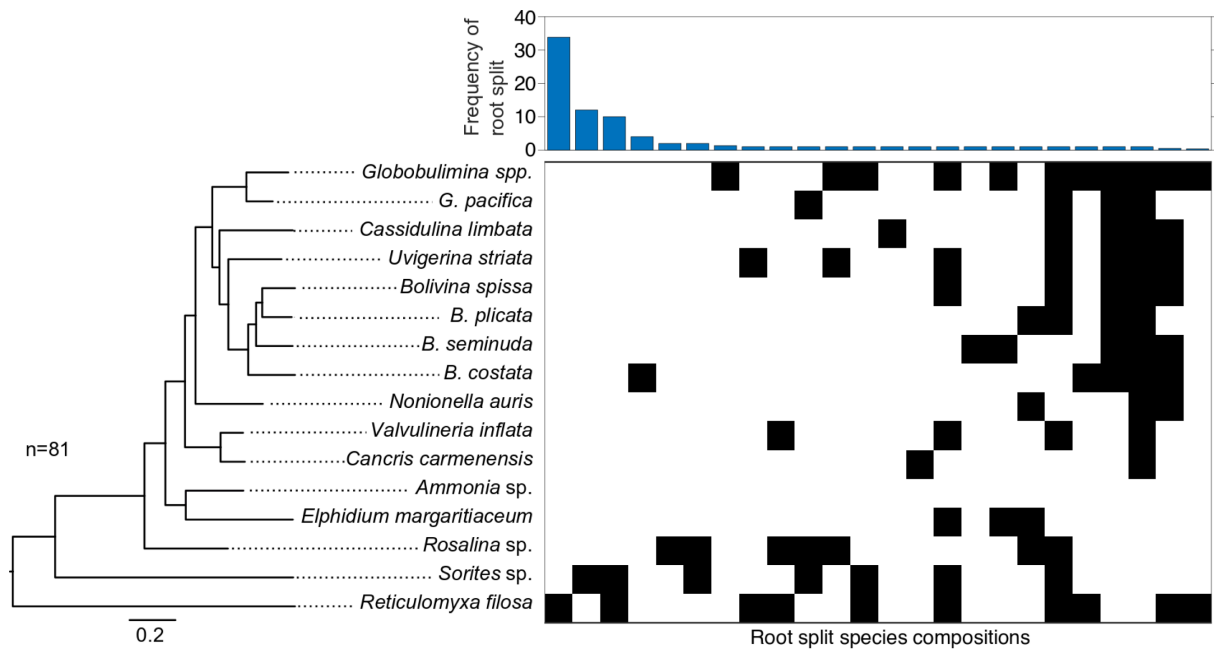
- 622 foraminifera revealed by 16S and aprA gene analysis. *Sci Rep* 1–12 (2019).
623 doi:10.1038/s41598-019-48166-5
- 624 26. Høgslund, S., Cedhagen, T., Bowser, S. S. & Risgaard-Petersen, N. Sinks and
625 Sources of Intracellular Nitrate in Gromiids. *Front Microbiol* **8**, 617 (2017).
- 626 27. Bernhard, J. M., Edgcomb, V. P., Casciotti, K. L., McIlvin, M. R. & Beaudoin, D. J.
627 Denitrification likely catalyzed by endobionts in an allogromiid foraminifer. *ISME J* **6**,
628 951–960 (2012).
- 629 28. Tria, F. D. K., Landan, G. & Dagan, T. Phylogenetic rooting using minimal ancestor
630 deviation. *Nat Ecol Evol* **1**, 0193 (2017).
- 631 29. Pawlowski, J. *et al.* The evolution of early Foraminifera. *Proc Natl Acad Sci USA* **100**,
632 11494–11498 (2003).
- 633 30. Ertan, K. T., Hemleben, V. & Hemleben, C. Molecular evolution of some selected
634 benthic foraminifera as inferred from sequences of the small subunit ribosomal DNA.
635 *Marine Micropaleontology* **53**, 367–388 (2004).
- 636 31. Mackensen, A., Schmiedl, G., Harloff, J. & Giese, M. Deep-Sea Foraminifera in the
637 South Atlantic Ocean: Ecology and Assemblage Generation. *Micropaleontology* **41**,
638 342 (1995).
- 639 32. Rathburn, A. E., Willingham, J., Ziebis, W., Burkett, A. M. & Corliss, B. H. A New
640 biological proxy for deep-sea paleo-oxygen: Pores of epifaunal benthic foraminifera.
641 *Sci Rep* **8**, 9456–8 (2018).
- 642 33. Hoogakker, B. A. A. *et al.* Glacial expansion of oxygen-depleted seawater in the
643 eastern tropical Pacific. *Nature* **562**, 410–413 (2018).
- 644 34. Widdel, F. New types of acetate-oxidizing, sulfate-reducing *Desulfobacter* species, *D.*
645 *hydrogenophilus* sp. nov., *D. latus* sp. nov., and *D. curvatus* sp. nov. *Arch. Microbiol.*
646 **148**, 286–291 (1987).
- 647 35. Lage, O. M. & Bondoso, J. Planctomycetes and macroalgae, a striking association.
648 *Front Microbiol* **5**, 267 (2014).
- 649 36. Oshiki, M., Satoh, H. & Okabe, S. Ecology and physiology of anaerobic ammonium
650 oxidizing bacteria. *Environ. Microbiol.* **18**, 2784–2796 (2016).
- 651 37. Noguchi, T. *et al.* *Vibrio alginolyticus*, a tetrodotoxin-producing bacterium, in the
652 intestines of the fish *Fugu vermicularis vermicularis*. *Marine Biology* **94**, 625–630
653 (1987).
- 654 38. McFall-Ngai, M. Divining the essence of symbiosis: insights from the squid-vibrio
655 model. *PLoS Biol.* **12**, e1001783 (2014).
- 656 39. Ben-Haim, Y., Zicherman-Keren, M. & Rosenberg, E. Temperature-regulated
657 bleaching and lysis of the coral *Pocillopora damicornis* by the novel pathogen *Vibrio*
658 *coralliilyticus*. *Appl. Environ. Microbiol.* **69**, 4236–4242 (2003).
- 659 40. López-Pérez, M. & Rodríguez-Valera, F. in *The Prokaryotes: Gammaproteobacteria*
660 (eds. Rosenberg, E., DeLong, E. F., Lory, S., Stackebrandt, E. & Thompson, F.) 69–92
661 (Springer Berlin Heidelberg, 2014).
- 662 41. Ivanova, E. P., Flavier, S. & Christen, R. Phylogenetic relationships among marine
663 Alteromonas-like proteobacteria: emended description of the family
664 Alteromonadaceae and proposal of Pseudoalteromonadaceae fam. nov.,
665 Colwelliaceae fam. nov., Shewanellaceae fam. nov., Moritellaceae fam. nov.,
666 Ferrimonadaceae fam. nov., Idiomarinaceae fam. nov. and Psychromonadaceae fam.
667 nov. *Int J Syst Evol Microbiol* **54**, 1773–1788 (2004).
- 668 42. Simon, M. *et al.* Phylogenomics of Rhodobacteraceae reveals evolutionary adaptation
669 to marine and non-marine habitats. *ISME J* **11**, 1483–1499 (2017).
- 670 43. Newton, R. J. *et al.* Genome characteristics of a generalist marine bacterial lineage.
671 *ISME J* **4**, 784–798 (2010).
- 672 44. Buchan, A., Gonzalez, J. M. & Moran, M. A. Overview of the marine roseobacter
673 lineage. *Appl. Environ. Microbiol.* **71**, 5665–5677 (2005).
- 674 45. Hjelm, M. *et al.* Selection and identification of autochthonous potential probiotic
675 bacteria from turbot larvae (*Scophthalmus maximus*) rearing units. *Syst. Appl.*
676 *Microbiol.* **27**, 360–371 (2004).

- 677 46. Webster, N. S., Negri, A. P., Munro, M. M. H. G. & Battershill, C. N. Diverse microbial
678 communities inhabit Antarctic sponges. *Environ. Microbiol.* **6**, 288–300 (2004).
- 679 47. Jain, C., Rodriguez-R, L. M., Phillippy, A. M., Konstantinidis, K. T. & Aluru, S. High
680 throughput ANI analysis of 90K prokaryotic genomes reveals clear species
681 boundaries. *Nat Commun* **9**, 5114–8 (2018).
- 682 48. Dubilier, N. *et al.* Endosymbiotic sulphate-reducing and sulphide-oxidizing bacteria in
683 an oligochaete worm. *Nature* **411**, 298–302 (2001).
- 684 49. Kamke, J. *et al.* Single-cell genomics reveals complex carbohydrate degradation
685 patterns in poribacterial symbionts of marine sponges. *ISME J* **7**, 2287–2300 (2013).
- 686 50. Wein, T. *et al.* Currency, Exchange, and Inheritance in the Evolution of Symbiosis.
687 *Trends Microbiol.* **27**, 836–849 (2019).
- 688 51. Strittmatter, A. W. *et al.* Genome sequence of *Desulfobacterium autotrophicum*
689 HRM2, a marine sulfate reducer oxidizing organic carbon completely to carbon
690 dioxide. *Environ. Microbiol.* **11**, 1038–1055 (2009).
- 691 52. González, P. J., Correia, C., Moura, I., Brondino, C. D. & Moura, J. J. G. Bacterial
692 nitrate reductases: Molecular and biological aspects of nitrate reduction. *J. Inorg.*
693 *Biochem.* **100**, 1015–1023 (2006).
- 694 53. Dias, J. M. *et al.* Crystal structure of the first dissimilatory nitrate reductase at 1.9 Å
695 solved by MAD methods. *Structure* **7**, 65–79 (1999).
- 696 54. Widdel, F. & Pfennig, N. Studies on dissimilatory sulfate-reducing bacteria that
697 decompose fatty acids II. Incomplete oxidation of propionate by *Desulfobulbus*
698 *propionicus* gen. nov., sp. nov. *Arch. Microbiol.* **131**, 360–365 (1982).
- 699 55. Berks, B. C., Ferguson, S. J., Moir, J. W. & Richardson, D. J. Enzymes and
700 associated electron transport systems that catalyse the respiratory reduction of
701 nitrogen oxides and oxyanions. *Biochim. Biophys. Acta* **1232**, 97–173 (1995).
- 702 56. Graf, J. S. *et al.* Anaerobic endosymbiont generates energy for ciliate host by
703 denitrification. *Nature* **591**, 445–450 (2021).
- 704 57. Duperron, S. *et al.* A dual symbiosis shared by two mussel species, *Bathymodiolus*
705 *azoricus* and *Bathymodiolus puteoserpentis* (Bivalvia: Mytilidae), from hydrothermal
706 vents along the northern Mid-Atlantic Ridge. *Environ. Microbiol.* **8**, 1441–1447 (2006).
- 707 58. Maklay, M. Novye Rannekamennougolnye Arkhedistsidy. *Min. Geol. Okhrana. Nedr.*
708 *USSR* **1**, 158–159 (1964).
- 709 59. Crespin, I. Permian Foraminifera of Australia. *Bur. Miner. Resour. Aust. Bull.* **48**, 1–
710 207 (1958).
- 711 60. Tappan, H. & Loeblich, A. R. Foraminiferal evolution, diversification, and extinction.
712 *Journal of Paleontology* **62**, 695–714 (1988).
- 713 61. Loeblich, A. R. & Tappan, H. *Treatise on Invertebrate Paleontology. Part C. Protista 2.*
714 *Sarcodina chiefly 'thecamoebians' and Foraminiferida.* (Geological Society of America
715 New York/University of Kansas Lawrence, 1964).
- 716 62. Kucera, M. & Schönfeld, J. The origin of modern oceanic foraminiferal faunas and
717 Neogene climate change. *The Micropalaeontology Society Special Publications* 409–
718 425 (2007).
- 719 63. Schlanger, S. O. & Jenkyns, H. C. Cretaceous oceanic anoxic events: causes and
720 consequences. *Geologie en Mijnbouw* **55**, 179–184 (1976).
- 721 64. Jenkyns, H. C. Cretaceous anoxic events: from continents to oceans. *Journal of the*
722 *Geological Society* **137**, 171–188 (1980).
- 723 65. Forde, B. G. Nitrate transporters in plants: structure, function and regulation. *Biochim.*
724 *Biophys. Acta* **1465**, 219–235 (2000).
- 725 66. Pao, S. S., Paulsen, I. T. & Saier, M. H. Major facilitator superfamily. *Microbiol. Mol.*
726 *Biol. Rev.* **62**, 1–34 (1998).
- 727 67. Sierra, R. *et al.* Deep relationships of Rhizaria revealed by phylogenomics: A farewell
728 to Haeckel's Radiolaria. *Mol Phylogenet Evol* **67**, 53–59 (2013).
- 729 68. Figueroa, S., Marchant, M., Giglio, S. & Ramírez, M. Foraminíferos bentónicos
730 rotalínidos del centro sur de Chile (36°S - 44°S). *Gayana* **69**, 329–363 (2005).

- 731 69. Erdem, Z. Reconstruction of past bottom water conditions of the Peruvian Oxygen
732 Minimum Zone (OMZ) for the last 22,000 years and the benthic foraminiferal response
733 to (de)oxygenation. *PhD thesis, Kiel University* (2016).
- 734 70. Mallon, J. Benthic Foraminifera of the Peruvian and Ecuadorian Continental Margin.
735 *PhD thesis, Kiel University* (2012).
- 736 71. Bolger, A. M., Lohse, M. & Usadel, B. Trimmomatic: a flexible trimmer for Illumina
737 sequence data. *Bioinformatics* **30**, 2114–2120 (2014).
- 738 72. Nurk, S. *et al.* Assembling single-cell genomes and mini-metagenomes from chimeric
739 MDA products. *J Comput Biol* **20**, 714–737 (2013).
- 740 73. Haas, B. J. *et al.* De novo transcript sequence reconstruction from RNA-seq using the
741 Trinity platform for reference generation and analysis. *Nat Protoc* **8**, 1494–1512
742 (2013).
- 743 74. Li, B. & Dewey, C. N. RSEM: accurate transcript quantification from RNA-Seq data
744 with or without a reference genome. *BMC Bioinformatics* **12**, 323 (2011).
- 745 75. Langmead, B. & Salzberg, S. L. Fast gapped-read alignment with Bowtie 2. *Nat*
746 *Methods* **9**, 357–359 (2012).
- 747 76. Simão, F. A., Waterhouse, R. M., Ioannidis, P., Kriventseva, E. V. & Zdobnov, E. M.
748 BUSCO: assessing genome assembly and annotation completeness with single-copy
749 orthologs. *Bioinformatics* **31**, 3210–3212 (2015).
- 750 77. Rice, P., Longden, I. & Bleasby, A. EMBOSS: the European Molecular Biology Open
751 Software Suite. *Trends Genet.* **16**, 276–277 (2000).
- 752 78. Katoh, K. & Standley, D. M. MAFFT multiple sequence alignment software version 7:
753 improvements in performance and usability. *Mol Biol Evol* **30**, 772–780 (2013).
- 754 79. Nguyen, L.-T., Schmidt, H. A., Haeseler, von, A. & Minh, B. Q. IQ-TREE: a fast and
755 effective stochastic algorithm for estimating maximum-likelihood phylogenies. *Mol Biol*
756 *Evol* **32**, 268–274 (2015).
- 757 80. Felsenstein, J. Cases in which parsimony or compatibility methods will be positively
758 misleading. *Systematic Zoology* **27**, 401–410 (1978).
- 759 81. Yilmaz, P. *et al.* The SILVA and ‘All-species Living Tree Project (LTP)’ taxonomic
760 frameworks. *Nucleic Acids Res* **42**, D643–8 (2014).
- 761 82. Morard, R. *et al.* PFR2: a curated database of planktonic foraminifera 18S ribosomal
762 DNA as a resource for studies of plankton ecology, biogeography and evolution.
763 *Molecular Ecology Resources* **15**, 1472–1485 (2015).
- 764 83. Altschul, S. F. *et al.* Gapped BLAST and PSI-BLAST: a new generation of protein
765 database search programs. *Nucleic Acids Res* **25**, 3389–3402 (1997).
- 766 84. Pruitt, K. D., Tatusova, T., Brown, G. R. & Maglott, D. R. NCBI Reference Sequences
767 (RefSeq): current status, new features and genome annotation policy. *Nucleic Acids*
768 *Res* **40**, D130–D135 (2012).
- 769 85. Li, W. & Godzik, A. Cd-hit: a fast program for clustering and comparing large sets of
770 protein or nucleotide sequences. *Bioinformatics* **22**, 1658–1659 (2006).
- 771 86. Mai, H. *et al.* AC-DIAMOND v1: accelerating large-scale DNA-protein alignment.
772 *Bioinformatics* **34**, 3744–3746 (2018).
- 773 87. Huson, D. H. *et al.* MEGAN Community Edition - Interactive Exploration and Analysis
774 of Large-Scale Microbiome Sequencing Data. *PLoS Comput Biol* **12**, e1004957
775 (2016).
- 776 88. Li, D., Liu, C.-M., Luo, R., Sadakane, K. & Lam, T.-W. MEGAHIT: an ultra-fast single-
777 node solution for large and complex metagenomics assembly via succinct de Bruijn
778 graph. *Bioinformatics* **31**, 1674–1676 (2015).
- 779 89. Wu, Y.-W., Simmons, B. A. & Singer, S. W. MaxBin 2.0: an automated binning
780 algorithm to recover genomes from multiple metagenomic datasets. *Bioinformatics* **32**,
781 605–607 (2016).
- 782 90. Parks, D. H., Imelfort, M., Skennerton, C. T., Hugenholtz, P. & Tyson, G. W. CheckM:
783 assessing the quality of microbial genomes recovered from isolates, single cells, and
784 metagenomes. *Genome Res* **25**, 1043–1055 (2015).

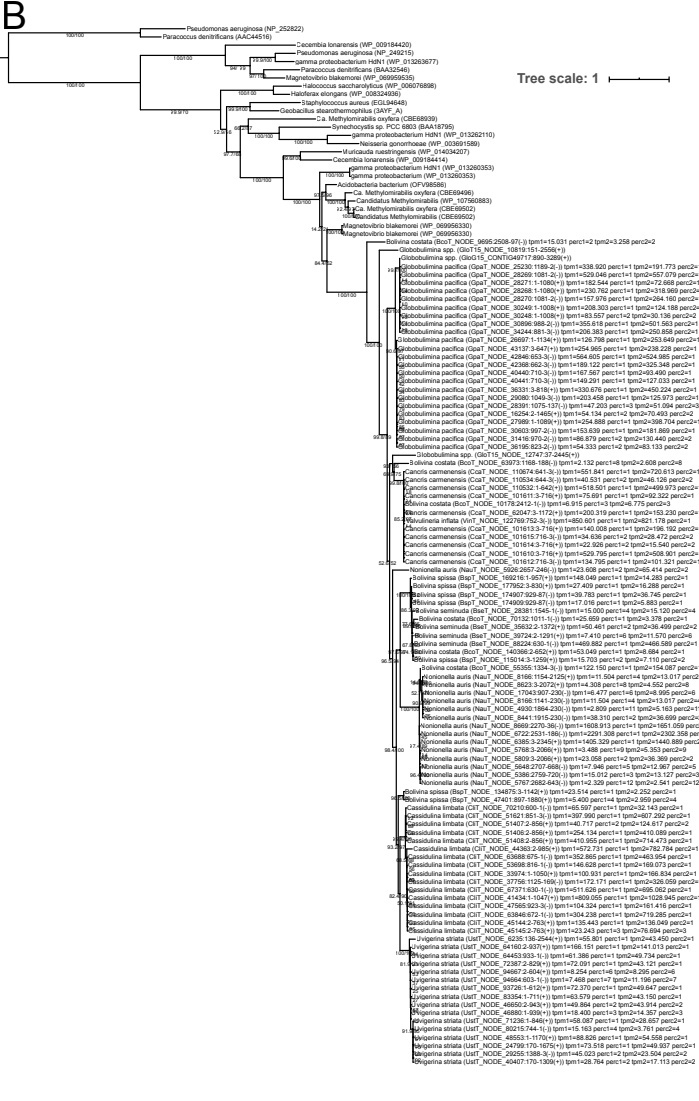
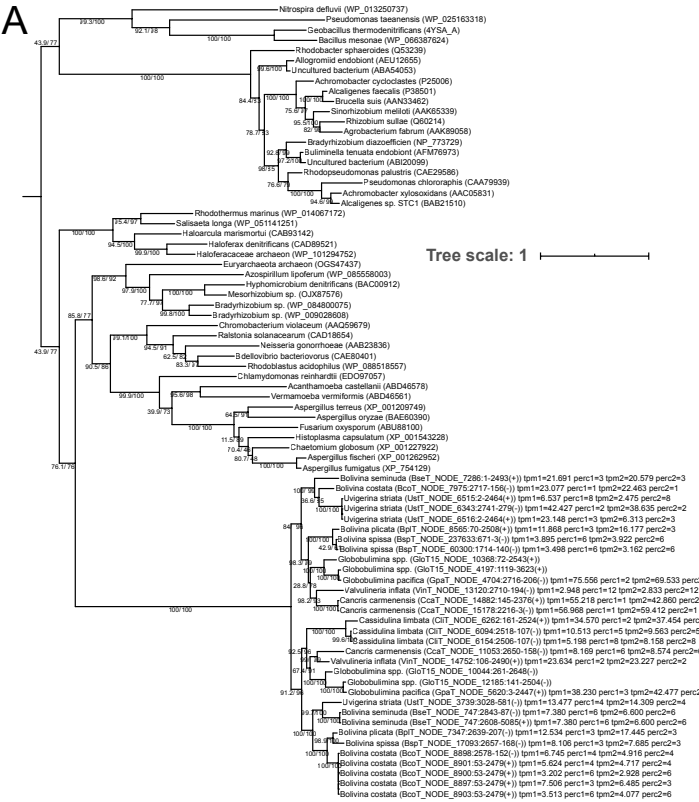
- 785 91. Tatusov, R. L., Koonin, E. V. & Lipman, D. J. A genomic perspective on protein
786 families. *Science* **278**, 631–637 (1997).
787 92. Enright, A. J., Van Dongen, S. & Ouzounis, C. A. An efficient algorithm for large-scale
788 detection of protein families. *Nucleic Acids Res* **30**, 1575–1584 (2002).
789 93. Huson, D. H. Application of phylogenetic networks in evolutionary studies. *Mol Biol*
790 *Evol* **23**, 254–267 (2005).
791 94. Moriya, Y., Itoh, M., Okuda, S., Yoshizawa, A. C. & Kanehisa, M. KAAS: an automatic
792 genome annotation and pathway reconstruction server. *Nucleic Acids Res* **35**, W182–
793 5 (2007).
794 95. Nielsen, H. Predicting Secretory Proteins with SignalP. *Methods Mol. Biol.* **1611**, 59–
795 73 (2017).
796
797
798

1 Supplementary material



2
3
4
5
6
7
8
9
10
11

Suppl. Figure S1. Foraminifera rooting based on single-protein trees. A Maximum-likelihood phylogenetic reconstruction of foraminifera species based on 81 eukaryotic protein marker sequences is shown on the left. Parametric bootstrap support is 1000/1000 at all the branches. Right of the phylogeny a split representation of root splits determined via the MAD approach for the 81 single gene trees is shown. Each column represents a root. Root branches are reported as separation of two groups (black and white boxes) indicating for the species found on either side of the root split. The bar graph (top) reports the single gene tree count supporting the corresponding root splits. These were ranked by frequency.

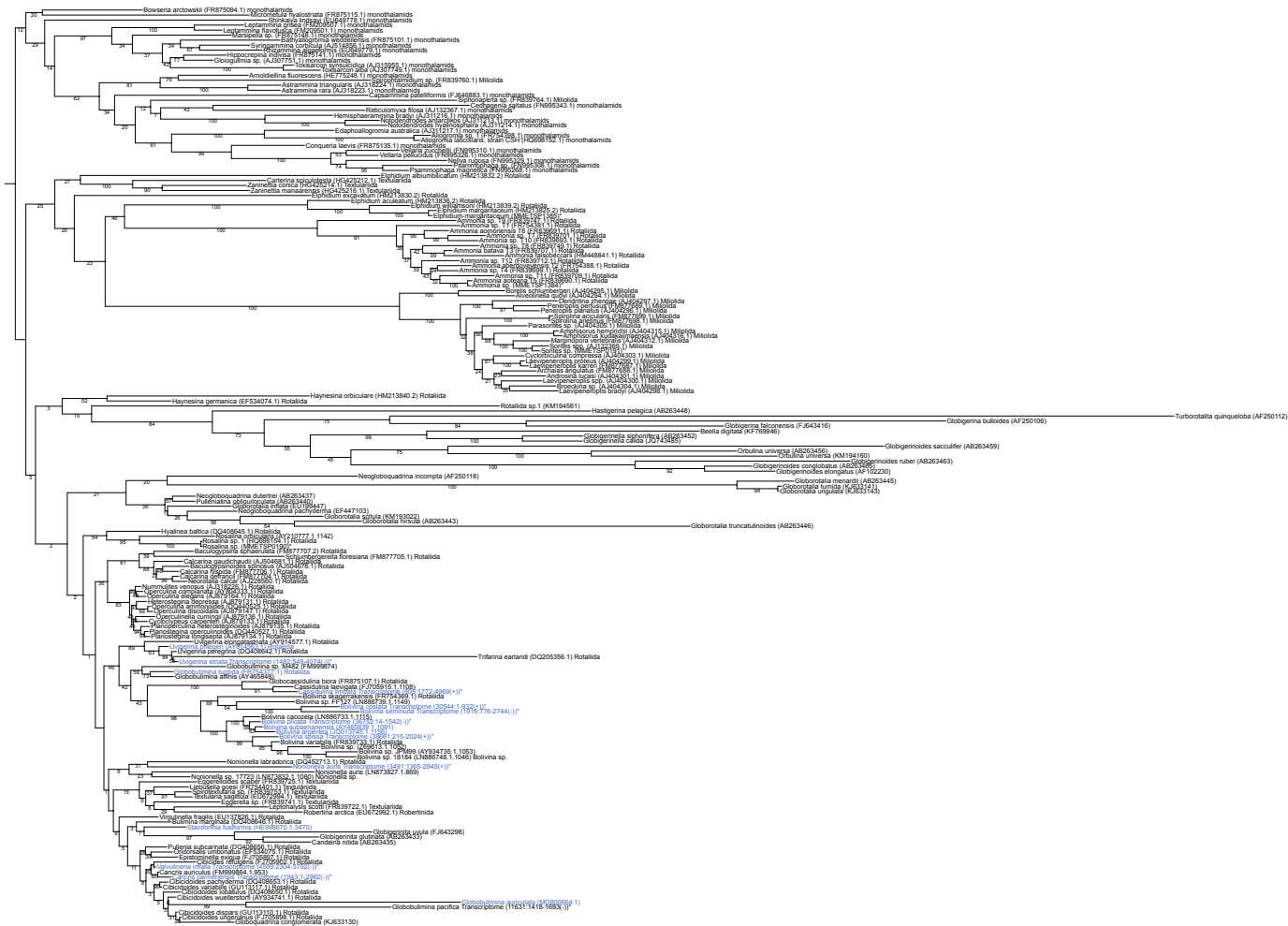




13

14 **Suppl. Figure S2. Complete phylogenies of NirK, Nor and Nrt homologs.** Phylogenetics
15 trees of the foraminiferal denitrification proteins A) NirK B) Nor and C) Nrt that survived the
16 cutoff together with homologs from public databases. Transcriptome labels contain
17 transcription values of the two replicates (tpm1 & tpm2) as well as their percentile expression
18 rank within corresponding transcriptomes. The labels contain as well the transcript id, region
19 and orientation for individual open reading frames used. Numbers of the branches represent
20 statistical support by ultrafast bootstrap and SH-like approximate likelihood ratio test results
21 (following the '/') each with 1000 replicates. Branch support values of zero are omitted. If only
22 one value is shown it represents the SH-like approximate likelihood ratio test.

Tree scale: 0.1



23

24

25

26

27

28

29

30

31

32

33

34

35

36

37

38

Suppl. Figure S3. Uncollapsed 18S phylogeny of foraminifera. Species shown to denitrify experimentally are highlighted in blue. The only exception is *Stainforthia fusiformis*, where denitrification activity has been shown for an unspecified species of the same genus. Species also shown in Figure 2 or Figure S1 are highlighted by asterisks. Bootstrap support values with 1000 replicates are shown at the branches. The trees were rooted by the clade of monothalamids containing *R. filosa*. The phylogeny corresponds to the one shown in Figure 3.

Suppl. Table S1. Sequencing statistics for metagenomics & transcriptomics.

Suppl. Table S2. List of foraminiferal homologs of denitrification proteins remaining after applying cutoffs.

Suppl. Table S3. List of foraminiferal homologs of denitrification proteins removed by cutoffs.

Suppl. Table S4. List of marker proteins used for phylogenetic reconstructions.

Suppl. Table S5. 18S sequences including metadata for phylogenetic reconstructions.

39 **Suppl. Table S6. Proportions of family rank classification of foraminifera-associated**
40 **microbial communities.**

41 **Suppl. Table S7. High quality genomic bins of foraminifera-associated species**
42 **communities.**

43 **Suppl. Table S8. Metabolic classification of Desulfobacteracea genomes.**

44